Experimental Study on Dynamic Splitting Tensile Failure Mode of Carbon Nanofibers Reinforced Concrete

Wei Xia[1], Jinyu Xu[1,2], Zhihang Wang[1], Zhe Huang[1], Gaojie Liu[1]
[1]College of Aeronautics Engineering, Air Force Engineering University, Xi'an, Shaanxi, 710038, China
[2]College of Mechanics and Civil Engineering, Northwestern Polytechnical University, Xi'an, Shaanxi, 710072, China

Abstract. Carbon nanofibers (CNFs) were used as admixtures to modify traditional concrete, and carbon nanofibers reinforced concrete (CNFC) with fiber volume fraction of 0%, 0.1%, 0.2%, 0.3% and 0.5% were prepared. The dynamic splitting tensile tests of concrete with different fiber volume contents under five loading rates were carried out by using the Φ100 mm split Hopkinson pressure bar (SHPB) test device. Based on the observation and analysis of the failure modes of the specimens, combined with the energy change rate of incident wave, the failure characteristics of CNFC under dynamic splitting tensile load are expounded. The results show that: the addition of CNFs has a certain inhibition effect on the dynamic splitting tensile failure of concrete; the failure modes of the specimens are the central failure along the loading direction; with the increase of the energy change rate of incident wave, the damage degree of the specimen is gradually aggravated.

1 Introduction

In recent years, with the continuous development of various high-performance, high-precision and high damage weapons, military protection engineering is facing more adverse factors such as stronger external stress, stronger weapon penetration, stronger explosion impact. In order to deal with the attack of modern high-damage weapons, the first measure is to develop and select new protective materials, and to build protective structures in the deep underground to resist the penetration of earth penetrating weapons.

At present, concrete is still the main material for building protective engineering. With the continuous progress of modern material science, especially the application of nanotechnology in various disciplines, it is possible to develop traditional concrete to high strength, high performance and multi-function. Carbon nanofibers (CNFs) are a form of carbon fibers grown in chemical vapor phase. They are a kind of discontinuous nanometer sized graphite fibers prepared by pyrolysis of gaseous hydrocarbons. The average diameter of CNFs is about 50 ~ 100 nm and the length is 0.5 ~ 100 μm [1-3]. At the same time, carbon nanofibers are small in size, low in density, high in strength, and have good toughness and excellent electrical and thermal conductivity. As the chemical properties of carbon nanofibers are relatively stable and will not react with the components in concrete, it can be used as an admixture to modify the traditional concrete, so as to prepare a new composite material, namely carbon nanofibers reinforced concrete (CNFC).

Scholars have done a lot of research on the compressive mechanical properties of concrete under dynamic load. With the deepening of the research, people pay more and more attention to the tensile properties of concrete materials, especially the tensile response of materials under dynamic load. For the protection engineering, most of the loads in wartime are strong loads such as explosion and impact, so it is necessary to carry out the experimental research on tensile failure of carbon nanofiber reinforced concrete under dynamic load. In view of this, the dynamic splitting tensile tests of CNFC were carried out by using the Φ100 mm split Hopkinson pressure bar (SHPB) test device, and its failure characteristics under the dynamic splitting tensile load were analyzed based on the failure mode.

2 Test

2.1 Test material

Qinling brand 42.5R ordinary portland cement; limestone gravel, unit weight is 2700 kg/m3, particle size range is 5-20 mm; Bahe natural medium sand, unit weight is 2630 kg/m3, fineness modulus is 2.78, bulk density is 1.50; JKPCA-02 FDN superplasticizer, produced by Shaanxi Haoyu concrete admixture Co., Ltd.; laboratory tap water; carbon nanofibers produced by Beijing daoking Co., Ltd.

2.2 Mix proportions of concrete body

The mix proportions of concrete body are shown in Table 1, where PC is the control group specimen without CNFs, and CNFC01, CNFC02, CNFC03, and CNFC05 are reinforced concrete specimens with 0.1%, 0.2%, 0.3% and 0.5% volume fraction of CNFs respectively. CNFC was

prepared by the method of wrapping sand and stone. The microstructure of concrete specimens was observed by FE-SEM field emission scanning electron microscope (Fig. 1) produced by FEI company of USA, as shown in Fig. 2.

Table 1. Mix proportions of concrete body (kg/m^3).

Specimen number	Cement	Gravel	Sand	Water	superplasticizer	CNFs
PC	495	1008	672	180	0	0
CNFC01	495	1008	672	180	5.0	0.18
CNFC02	495	1008	672	180	7.5	0.36
CNFC03	495	1008	672	180	10.0	0.54
CNFC05	495	1008	672	180	15.0	0.90

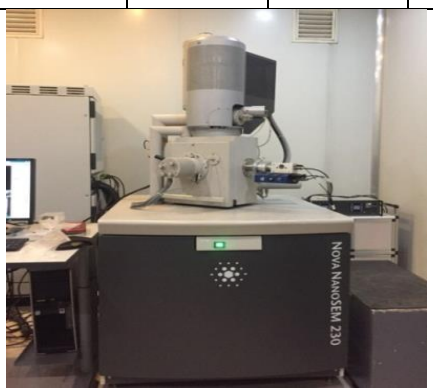

Figure. 1. FE-SEM field emission scanning electron microscope.

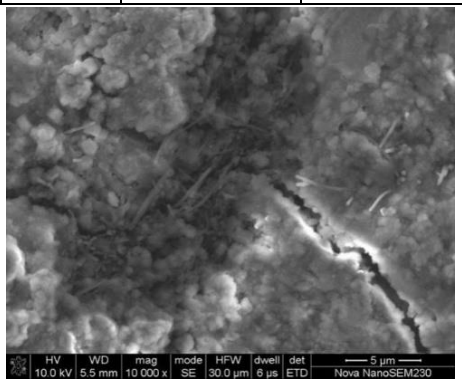

Figure. 2. Typical microstructure of CNFC.

2.3 Test principle

Based on the SHPB test device, the dynamic splitting tensile tests of CNFC was carried out. The specimen was initially designed as a Φ100 mm × 50 mm short cylinder, and then polished into a flattened Brazilian disc with a platform central angle of 2α = 20 ° (Fig. 3). According to the literature search, this test method is easy to operate and has mature theory, and can simulate the tensile mechanical response of materials under dynamic load [9-14].

Five strain rate levels were set in the test. The strain rate reflects the impact velocity. According to the existing research results, it can be found that the two are almost linear. The impact velocity is controlled by the applied air pressure and the air pressure action distance. During the test, the action distance of air pressure remains unchanged, and the impact speed is controlled by controlling the input air pressure, as shown in Fig. 4. It should be noted that although the impact velocity of the striker is controlled by the input air pressure and the action distance of the air pressure, the test environment will also have an impact on it. At the same time, after the continuous test of the equipment, the temperature of the launcher and the firing barrel will slightly change, and these temperature changes will have a certain impact on the internal air pressure. Therefore, although the input air pressure and the working distance of the air pressure can be kept constant, the impact velocity of the striker is difficult to ensure the same every time (the strain rate will be slightly different under the same controllable launching conditions).

Fig. 5 is the schematic diagram of stress wave propagation in dynamic splitting tensile test. During the test, make sure that the two platform surfaces of the specimen are located at the center of the end face of the bar and closely fit with the bar. When the striker impacts the incident bar, the incident pulse ($\varepsilon_I(t)$) is generated in the rod. When ($\varepsilon_I(t)$) passes through the interface A, part of it is reflected to form the reflection pulse ($\varepsilon_R(t)$), and the other part is transmitted into the transmission bar through the specimen to form the transmission pulse ($\varepsilon_T(t)$). In the process of dynamic splitting tensile test, the contact surface between the specimen and the incident bar and the transmission bar is small, and the stress wave that can be transmitted to the specimen in the incident bar is very small. After the reflection of the specimen, the stress wave signal that can be received in the transmission bar is very small, only about one tenth of the incident pulse. With the continuous improvement of SHPB test technology, especially the progress of strain signal acquisition system, transmission strain can be effectively collected, and the mutual interference between incident signal and reflected signal can be ignored. Therefore, the “three wave method” based on incident wave, reflected wave and transmitted wave can still effectively calculate the stress state of specimen under dynamic splitting tension load.

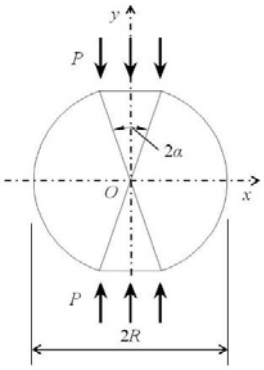

Figure. 3. Schematic diagram of flattened Brazilian disc.

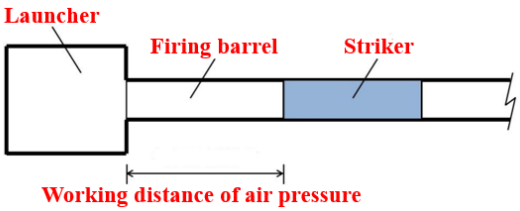

Figure. 4. Control of impact speed.

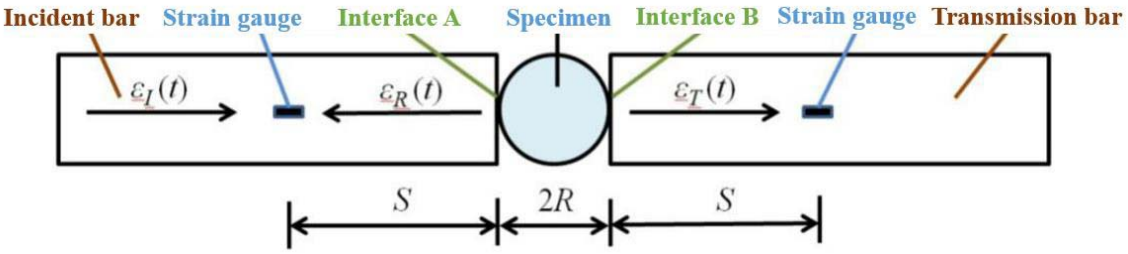

Figure. 5. Schematic diagram of stress wave propagation.

3 Test results and analysis

3.1 Energy change rate of incident wave

The energy change rate of incident wave ($\dot{W}_I$) is defined as the ratio of total incident wave energy WI(t) to stress wave propagation time (τ). The value of $\dot{W}_I$ can reflect the action speed of the incident energy and the strength of the dynamic splitting tensile load on the specimen.

$$\dot{W}_I = W_I(t)/\tau$$

Table 3 and table 4 show the change rate of incident wave energy obtained from dynamic splitting tensile test after being processed by "three wave method".

Table 2. Dynamic splitting tensile test results of PC group specimens.

PC	Number	1	2	3	4	5
	$\bar{\dot{\varepsilon}}$ (s^{-1})	15.21	19.62	25.87	28.96	31.42
	$\dot{W}_I$ ($MJ \cdot s^{-1}$)	0.136	0.504	0.978	1.343	1.877

Table 3. Dynamic splitting tensile test results of CNFC group specimens.

CNFC01	Number	1	2	3	4	5
	$\bar{\dot{\varepsilon}}$ (s^{-1})	14.75	19.16	26.71	30.29	34.13
	$\dot{W}_I$ ($MJ \cdot s^{-1}$)	0.142	0.377	0.955	1.728	2.081
CNFC02	Number	1	2	3	4	5
	$\bar{\dot{\varepsilon}}$ (s^{-1})	15.38	23.26	28.61	31.89	35.07
	$\dot{W}_I$ ($MJ \cdot s^{-1}$)	0.145	0.601	1.729	2.113	2.606
CNFC03	Number	1	2	3	4	5
	$\bar{\dot{\varepsilon}}$ (s^{-1})	16.72	18.73	28.64	32.78	36.43
	$\dot{W}_I$ ($MJ \cdot s^{-1}$)	0.203	0.353	1.726	2.262	2.781
CNFC05	Number	1	2	3	4	5
	$\bar{\dot{\varepsilon}}$ (s^{-1})	15.65	18.02	20.37	25.69	30.29
	$\dot{W}_I$ ($MJ \cdot s^{-1}$)	0.163	0.272	0.401	0.907	2.219

3.2 Analysis of failure mode

The failure mode is the most intuitive reflection of concrete under external load, and the failure modes of each group of specimens under dynamic splitting tensile

load are shown in Fig. 6 and Fig. 7. It can be seen from the observation that the failure modes of each group of specimens are basically the same, all of them are the central failure along the loading direction; in PC group, the specimens are brittle due to the lack of fiber, and the failure is serious even in lower $\dot{\varepsilon}$ (19.62 s^{-1}); as a whole, with the increase of $\dot{\varepsilon}$, the damage of the specimen gradually intensifies. For example, in the case of lower $\dot{\varepsilon}$ (15.38 s^{-1}), the damage of the specimen is basically divided into two parts along the direction of the main crack, and the damage of the rest parts is very small. When $\dot{\varepsilon}$ (23.26 s^{-1}) is raised, the specimen begins to appear a similar "inverted triangle" shape damage at the platform end; with the further increase of $\dot{\varepsilon}$ (35.07 s^{-1}), not only the damage at the platform end increases, but also the two ends of the main crack appear serious damage.

From the analysis of the damage degree, it can be seen that with the increase of the change rate of incident wave energy ($\dot{W}_I$), the damage degree of the specimen is more serious; from the aspect of failure form, when $\dot{W}_I$ is small, the specimen breaks into two parts, with less local damage. However, with the increase of $\dot{W}_I$, the comminution of the specimen in the loading end, i.e. the platform, is similar to the triangle area. The larger the $\dot{W}_I$ is, the larger the area of the comminution area is, and the comminution area of the specimen in contact with the incident bar is larger than that of the transmission bar.

The external energy acting on the specimen is the direct cause of the internal crack generation, extension and macro failure of the concrete. The formation, propagation, initiation, extension, penetration and merger of the cracks need to absorb energy from the outside at each stage, and it is an irreversible energy dissipative process. Therefore, from the perspective of energy dissipative, the failure mode of dynamic splitting tension can be well explained: when the energy carried by the incident wave is low, the dissipated energy of the specimen is only enough for the evolution of a few cracks in the loading center, and the level of macro fracture is not obvious; with the increase of the energy carried by the incident wave, the dissipated energy also increases, when the energy is increased to enable the development of other cracks and the formation of the main crack, the radial fracture occurs in the specimen, the local damage is small; the energy carried by the incident wave continues to increase, and the dissipated energy of the specimen is more and more, while the main crack is formed, the micro-cracks in the surrounding area can develop and participate in the failure process, resulting in the formation of a similar triangle crushing area.

Figure. 6. Typical failure mode of PC group specimens.

(a) CNFC01 group

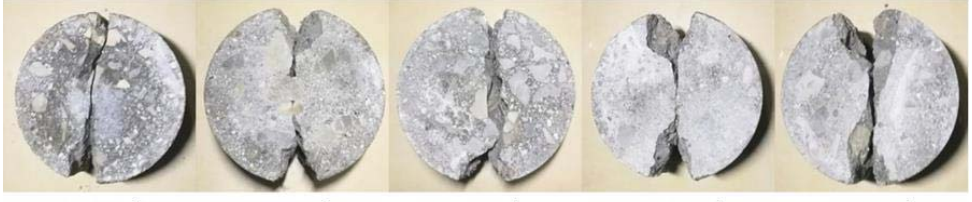

(b) CNFC02 group

(c) CNFC03 group

(d) CNFC05 group

Figure. 7. Typical failure mode of CNFC group specimens.

4 Conclusion

In this paper, CNFs were used as additives to modify traditional concrete to prepare CNFC. The dynamic splitting tensile tests of CNFC specimens with fiber volume fraction of 0%, 0.1%, 0.2%, 0.3% and 0.5% were carried out by using Φ100 mm SHPB test device. Based on the observation and analysis of the failure modes of the specimens, combined with the energy change rate of incident wave, the failure characteristics of concrete under dynamic splitting tensile load are expounded. The main conclusions are as follows:

（1）The addition of CNFs has a certain inhibition effect on the dynamic splitting tensile failure of concrete.

（2）The failure modes of the specimens are basically the same, and all of them are the central failure along the loading direction.

（3）With the increase of incident wave energy change rate, the damage degree of the specimen is gradually intensified, and the area of triangular crushing area at the loading end is larger.

References

1. Zhao J. Carbon nanofiber and it's applications[J]. Hi-Tech Fiber and Application, 2003, 28(2): 7-10. (in Chinese).
2. Zheng J, Zhang X, Li P, et al. Application of carbon nanofibers in chemical power source[J]. Chinese Journal of Power Sources, 2011, 35(8): 1028-1030.(in Chinese)
3. Celebi S, Nijhuis T A, Van der Schaaf J, et al. Carbon nanofiber growth on carbon paper for proton exchange membrane fuel cells[J]. Carbon, 2011, 49(2): 501-507.
4. Zhang S, Song R, Wang C, et al. Experimental Investigation of the Compressive Behavior of RCC under High Strain Rates: Considering the Rolling Technique and Layered Structure[J]. Journal of Materials in Civil Engineering, 2018, 30(4): 04018057.
5. Ma Q, Gao C. Effect of Basalt Fiber on the Dynamic Mechanical Properties of Cement-Soil in SHPB Test[J]. Journal of Materials in Civil Engineering, 2018, 30(8): 04018185.
6. Lee S, Kim K M, Park J, et al. Pure rate effect on the concrete compressive strength in the split Hopkinson pressure bar test[J]. International Journal of Impact Engineering, 2018, 113: 191-202.
7. Ren W, Xu J, Su H. Dynamic compressive behavior of basalt fiber reinforced concrete after exposure to elevated temperatures[J]. Fire and materials, 2016, 40(5): 738-755.
8. Su H, Xu J. Dynamic compressive behavior of ceramic fiber reinforced concrete under impact load[J]. Construction and Building Materials, 2013, 45: 306-313.
9. Luo X, Xu J. Dynamic splitting-tensile testing of highly fluidised geopolymer concrete [J]. Magazine of Concrete Research, 2013, 65(14): 837-843.
10. Lambert D E, Ross C A. Strain rate effects on dynamic fracture and strength [J]. International Journal of Impact Engineering, 2000, 24(10): 985-998.
11. Chen X, Ge L, Yuan H, et al. Effect of Prestatic Loading on Dynamic Tensile Strength of Concrete under High Strain Rates[J]. Journal of Materials in Civil Engineering, 2016, 28(12): 06016018.
12. Wang Q Z, Jia X M, Kou S Q, et al. The flattened Brazilian disc specimen used for testing elastic modulus, tensile strength and fracture toughness of brittle rocks: Analytical and numerical results[J].

International Journal of Rock Mechanics and Mining Sciences, 2004, 41(2): 245-253.

13. Chen X, Ge L, Chen C, et al. Influence of Initial Static Splitting Tensile Loading on Dynamic Compressive Strength of Concrete Cores under High Strain Rates[J]. Journal of Performance of Constructed Facilities, 2016, 30(6): 06016002.
14. Feng W, Liu F, Yang F, et al. Experimental study on dynamic split tensile properties of rubber concrete[J]. Construction and Building Materials, 2018, 165: 675-687.